Contribution from the Laboratoire de Chimie des Solides, IPCM, 2 Rue de la Houssinière, 44072 Nantes Cedex 03, France

Split Model Description of the Copper Site Distribution in the New Layered (2D) $Cu^{I}V^{III}P_2S_6$ Phase

E. Durand, G. Ouvrard, M. Evain,* and R. Brec

Received January 26, 1990

$CuVP_2S_6$ has been obtained as single crystals from the elements at 500 °C in evacuated silica tubes. It crystallizes in the monoclinic symmetry, space group $C2$, with the cell parameters a = 594.62 (8) pm, b = 1029.9 (1) pm, c = 668.70 (6) pm, β = 107.247 (9)°, V = 391.1 (1) × 10^6 pm^3, and Z = 2. The refinement, in a split model approach, was carried out down to a reliability factor value R = 3.3% from 637 independent reflections and 72 variables. The structure is of the $M^{I}M^{III}P_2S_6$ type (i.e., derived from the $M^{II}{}_2P_2S_6$ structure) with a triangular cationic arrangement. Copper(I) ions do not occupy every other M^{II} octahedron as vanadium(III) cations do; they are distributed on three different crystallographic sites inside and outside the octahedra and present high thermal parameters.

Introduction

In 1965 Hahn and Klingen reported[1] the existence of a new family in the M-P-S system: the two-dimensional (2D) $M_2P_2S_6$ phases, where M is a bivalent metal. A few years ago, Leblanc and Rouxel[2a] and then Colombet et al. enlarged that family with the successful substitution of the M^{II} cations by (M^{I},M^{III}) couples.[2b,3] For their first trial, these authors chose the (Cu^{I},Cr^{III}) and (Ag^{I},Cr^{III}) couples on account of the great stability of the trivalent chromium in octahedral sites. After observing the occurrence of a V^{III}/V^{II} mixed valence in $V_{0.78}PS_3$,[4] it was thought possible to stabilize vanadium in the III oxidation state through the combination (Ag^{I},V^{III}) in an $M^{I}M^{III}P_2S_6$ compound. Indeed, $AgVP_2S_6$ could be synthesized,[5] as well as its seleno-equivalent $AgVP_2Se_6$.[6] Other silver phases (e.g., $AgScP_2S_6$ and $AgInP_2S_6$) were also prepared.[7,8] Beyond the interest of constituting a new class of layered materials, the $M^{I}M^{III}P_2S_6$ phases distinguish themselves by the special internal arrangement of the cations that determines some physical characteristics such as the magnetic behavior. The main structural features of the up-to-date series of known $M^{I}M^{III}P_2S_6$ phases are gathered in Table I. The different cationic arrangements (e.g., triangular or linear) found within the structure slabs have been correlated to the cation-chalcogen bond distance ratios;[9] triangular arrangements relate to the smallest ratios (close to but larger than 1) whereas linear ones correspond to the largest ratios. For cations of different enough sizes, the structural constraints would override the Coulombic repulsion and therefore favor chain patterns. Such an arrangement implies a symmetry lowering (space group $P2/a$) and a distortion in the sulfur atom planes. Correlatively, the b/a parameter ratio, which has the $\sqrt{3}$ ideal value in $M_2P_2S_6$,[10] shifts to higher values (i.e., 1.804).

The cation pattern confers special physical and crystallographical properties on the materials. For instance, the chromium and vanadium chain arrangement gives the $AgCrP_2S_6$ and $AgVP_2S_6$ compounds unusual magnetic characteristics in relation to antiferromagnetic coupling in the transition-metal chains.[3,5] $AgVP_2S_6$ is thus a very nice example illustrating the Haldane conjecture.[11] The AB-mode stacking of sulfur atoms in $AgInP_2S_6$ and $AgScP_2S_6$ allows a trigonal description of their structures.

The physical properties, in particular the magnetic ones, justify the efforts developed recently in the synthesis and characterization of new $M^{I}M^{III}P_2S_6$ phases. In this article are reported the preparation and the structural determination of $CuVP_2S_6$ along with some of its magnetic properties.

Experimental Section

Synthesis and Analysis. The heating at 500 °C for 2 weeks, in silica evacuated tubes, of a stoichiometric mixture of elemental copper, vanadium, phosphorus, and sulfur gave rise to a bunch of well-crystallized gray platelets embedded in an inhomogeneous bulk. The analysis of the crystals by means of STEM confirmed, within experimental accuracy, the $CuVP_2S_6$ stoichiometry. A complete X-ray investigation (vide infra) revealed the presence, in the main, of Cu_3PS_4.[12] Different attempts to produce pure, homogeneous bulk $CuVP_2S_6$ were unsuccessful, to date.

X-ray Powder Data. To minimize the amount of Cu_3PS_4 impurities, small $CuVP_2S_6$ crystals were carefully selected and randomly oriented on a thin, grease-covered, glass fiber. The sample, held on a goniometric head, was then set on an INEL diffractometer equipped with a CPS120 curve detector for room-temperature data recording. The diffraction pattern could be easily indexed starting with the typical $M_2P_2S_6$ lattice constants. A least-squares refinement ($\delta 2\theta_{av}$ = 0.014°) of the parameters of the C-centered monoclinic cell led to a = 594.62 (8) pm, b = 1029.9 (1) pm, c = 668.70 (6) pm, β = 107.247 (9)°, V = 391.1 (1) × 10^6 pm^3, and Z = 2. The indexed diffraction pattern (hkl assignment along with intensities calculated from the Lazy Pulverix program[13]) is given in Table II. Fourteen weak lines, not taken into account in that indexation, were found to match the major peaks of the Cu_3PS_4 powder diffraction pattern. The b/a ratio (1.732 ≈ $\sqrt{3}$) and the good agreement between the $\cos^{-1}(-a/3c)$ value and β (107.24° ≈ 107.23°) indicate an almost ideal packing arrangement.[10] The $CuVP_2S_6$ cell volume (391.1 × 10^6 pm^3) perfectly fits in between that of $CuCrP_2S_6$ (388.46 × 10^6 pm^3, when reduced to the same formula unit) and that of $AgVP_2S_6$ (409.5 × 10^6 pm^3) if we consider that Cr^{III} is smaller than V^{III} (radius of 61.4 vs 63 pm) and that Ag^{I} is larger than Cu^{I} (radius of 91 vs 77 pm).

Single-Crystal Studies. Weissenberg tests were carried out to select suitable crystals, which were then mounted in 0.3-mm Lindemann capillaries. A complete study on films to determine the symmetry and parameters values was then undertaken. It confirmed the occurrence of a monoclinic cell of the $M_2P_2S_6$ type. No superstructure could be found. A complementary electron diffraction work showed no extra peak either. Reflection intensities were measured on an Enraf-Nonius CAD4-κ diffractometer (1) for a trial, large single crystal without imposing extinction conditions (the reflections of intensities with $I > 3\sigma(I)$ left only the reflections corresponding to C centering) and (2) for a much smaller crystal (≈0.24 × 0.16 × 0.03 mm^3) in the $-h/h$, $0/k$, and $-l/l$ space portion, omitting systematic null reflections due to C centering. Hereinafter, it is the second recording we refer to. Mo Kα radiation and a graphite monochromator were used (cf. Table III). The cell parameters (a = 596.4 (4) pm, b = 1032.7 (11) pm, c = 671.0 (2) pm, and β = 107.21 (1)°) obtained from the 24 reflections selected for the crystal orientation were in reasonable agreements with those refined from the

(1) Hahn, H.; Klingen, W. *Natürwissenchaften* **1965**, *52*, 494.
(2) (a) Leblanc, A.; Rouxel, J. *C. R. Acad. Sci. Paris* **1980**, *C291*, 12, 263. (b) Colombet, P.; Leblanc, A.; Danot, M.; Rouxel, J. *J. Solid State Chem.* **1982**, *41*, 174.
(3) Colombet, P.; Leblanc, A.; Danot, M.; Rouxel, J. *Nouv. J. Chim.* **1983**, *7*, 333.
(4) Ouvrard, G.; Fréour, R.; Brec, R.; Rouxel, J. *Mater. Res. Bull.* **1985**, *20*, 1053.
(5) Lee, S.; Colombet, P.; Ouvrard, G.; Brec, R. *Mater. Res. Bull.* **1986**, *21*, 917.
(6) Ouvrard, G.; Brec, R. *Mater. Res. Bull.* **1988**, *23*, 1199.
(7) Lee, S.; Colombet, P.; Ouvrard, G.; Brec, R. *Inorg. Chem.* **1988**, *27*, 1291.
(8) Ouili, Z.; Leblanc, A.; Colombet, P. *J. Solid State Chem.* **1987**, *66*, 86.
(9) Colombet, P. Thesis, Nantes, France, 1982.
(10) Ouvrard, G.; Brec, R. *Eur. J. Solid State Inorg. Chem.* **1990**, *27*, 477.
(11) Mutka, H.; Soubeyroux, J. L.; Bourleaux, G.; Colombet, P. *Phys. Rev.* **1989**, *B39*, 4820.
(12) Garin, J.; Parthé, E. *Acta Crystallogr., Sect. B* **1972**, *B28*, 3672.
(13) Yvon, R.; Jeitschko, W.; Parthé, E. *J. Appl. Crystallogr.* **1977**, *10*, 73.

0020-1669/90/1329-4916$02.50/0

Table I. Essential $M^{I}M^{III}P_2X_6$ (X = S, Se) Structural Characteristics

	$V_{0.78}PS_3$[4]	$AgVP_2S_6$[5]	$AgCrP_2S_6$[3]	$AgVP_2Se_6$[6]	$AgScP_2S_6$[7]	$AgInP_2S_6$[8]	$CuCrP_2S_6$[2]
params							
a, pm	586.7 (1)	592.1 (1)	589.2 (3)	633.99 (6)	617.36 (6)	618.2 (2)	591.6 (1)
b, pm	1016.0 (2)	1068.4 (2)	1063.2 (4)	1102.0 (1)	617.36	618.2	1024.6 (2)
c, pm	665.7 (1)	675.5 (1)	674.5 (4)	698.19 (6)	1289.7 (2)	1295.7 (2)	1341.5 (5)
β, deg	107.08 (2)	106.62 (2)	105.88 (4)	106.824 (8)			107.09 (3)
V, 10^6 pm^3	379.3 (4)	409.5 (2)	406.4 (3)	466.9 (1)	425.7 (2)	428.8 (4)	776.9 (2)
space group	$C2/m$	$P2/a$	$P2/a$	$C2$	$P\bar{3}1c$	$P\bar{3}1c$	$C2/c$
b/a ratio	1.732	1.804	1.804	1.738	ideal	ideal	1.731
$\cos^{-1}(-a/3c)$	107.08	106.99	106.93	107.67			107.10
anionic stacking mode	ABC	ABC	ABC	ABC	AB	AB	ABC
cationic ordering	honeycomb	chain	chain	triangle	triangle	triangle	triangle
$D = r(M^{III}\text{-}X)$, pm	250.4	247	243	258	259	265	244
$d = r(M^{I}\text{-}X)$, pm		278	281	287	279	278	264
d/D ratio		1.13	1.16	1.11	1.07	1.05	1.06

Table II. X-ray Powder Diffraction of $CuVP_2S_6$

d_{obs}, pm	d_{calc}, pm	*hkl*	I_{calc}[a]
319.1	319.3	002	65.1
294.0	293.8 293.8	130 20$\bar{1}$	57.6
284.1	284.0 284.0	13$\bar{1}$ 200	19.9
252.7	252.6 252.6	131 20$\bar{2}$	100.0
186.5	186.5 186.5	13$\bar{3}$ 202	15.0
171.7	171.7 171.7	060 33$\bar{1}$	48.8
161.1	161.1 161.1	133 20$\bar{4}$	17.0
159.62	159.66	004	5.5
151.15	151.20 151.19 151.19	33$\bar{3}$ 062 331	23.8
141.97	141.98 141.97	26$\bar{2}$ 400	9.7
117.42	117.45 117.44	26$\bar{4}$ 402	4.7
116.90	116.91 116.91 116.90	33$\bar{5}$ 064 333	7.5
111.09	111.08 111.07	20$\bar{6}$ 135	7.5

[a] Intensities calculated with the Lazy Pulverix program[13] for a Debye–Scherrer geometry and without anomalous dispersion.

Table III. Crystallographic Data for $CuVP_2S_6$

$CuVP_2S_6$	M_r = 368.81
a = 594.62 (8) pm	space group $C2$ (No. 5)
b = 1029.9 (1) pm	λ = 0.71073 Å (Mo Kα)
c = 668.70 (6) pm	ρ_{calc} = 3.125 g/cm^3
β = 107.247 (9)°	μ = 57 cm^{-1}
V = 391.1 (1) × 10^6 pm^3	$R(F_o)$[a] = 0.033
Z = 2	$R_w(F_o)$[b] = 0.040
T = 291 K	

[a] $R = \sum(|F_o| - |F_c|)/\sum|F_o|$. [b] $R_w = (\sum w(|F_o| - |F_c|)^2/\sum wF_o^2)^{1/2}$.

powder data. After the usual reduction (including Lorentz polarization) of the 1814 raw data, a set of 637 independent reflections with $I > 3\sigma(I)$ were available for structure refinements. Although the absorption coefficient of $CuVP_2S_6$ was low (μ = 57 cm^{-1}), the shape of the crystal lead us to apply a Gaussian absorption correction. This resulted in no improvement of the final reliability factor (vide infra), and the corrections were disregarded.

Structure Refinement

All structure refinements and calculations were carried out with the SDP-Plus package (1982 version[14]). With the purpose of looking for an ordered distribution of the cations, the only suitable space group to select was the $C2$ group. Furthermore, the C mode implied a triangular distribution of the copper, vanadium, and phosphorus atoms. Thus, the first refinements were performed starting with that arrangement. The model proved correct, and after a few cycles and introduction of the anisotropic thermal factors the reliability factor (R) dropped to 6.5%. However, the results showed that the copper atom, in its octahedral site, presented abnormaly high thermal motion perpendicular to the *ab* plane. It was then decided to remove that position and to refine the remaining ones isotropically to prevent any directionally biased calculation. Hence, a difference Fourier map was calculated; it revealed, as shown in Figure 1, the presence of three independent maxima of different importance in each intraslab empty octahedra. After introduction of copper atoms on those positions, with fixed and then freed appropriate occupancy factors, R = 3.3%. At this point, a new difference Fourier map calculation did not show any significant features. The final atomic coordinates and equivalent isotropic thermal parameters are gathered in Table IV, and the main distances and angles for $CuVP_2S_6$ are listed in Table V. Since $C2$ is an acentric group, refinements were carried out by using $(1 - x)$

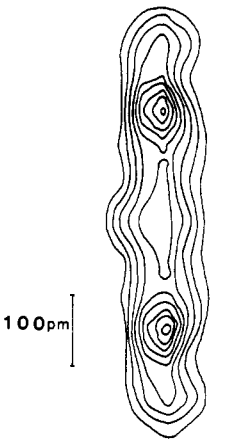

Figure 1. (−1,0,3) section of the difference Fourier map of $CuVP_2S_6$ before the introduction of copper atoms in the structure refinement. Three nonequivalent positions clearly show up: Cu1 in the center, Cu2 in the middle (predominant maximum), and Cu3 on the outside. Contour lines: 1.0, 1.5, ..., 5.0 × 10^{-6} e/pm^3.

Table IV. Positional and Thermal Parameters and Their Estimated Standard Deviations

atom	*x*	*y*	*z*	$10^{-4}B_{eq}$[a]	τ[b]
V	0	0.3308 (2)	0	1.23 (2)	
P	0.9442 (3)	0	0.8303 (2)	0.94 (2)	
S1	0.7270 (3)	0.6708 (2)	0.2539 (3)	1.31 (2)	
S2	0.2666 (2)	0.8418 (2)	0.2493 (2)	1.34 (2)	
S3	0.7476 (3)	0.4865 (2)	0.7510 (2)	1.28 (2)	
Cu1	0.970 (1)	0.673 (1)	0.012 (2)	4.6 (3)	0.139 (3)
Cu2	0.0693 (6)	0.6667 (5)	0.215 (1)	4.5 (1)	0.265 (3)
Cu3	0.126 (2)	0.669 (2)	0.371 (3)	2.3 (3)	0.066 (3)

[a] Isotropic equivalent thermal parameter defined as B_{eq} (pm^2) = $^4/_3$ $\sum_i\sum_j\beta_{ij}a_ia_j$. [b] Multiplicity times occupancy ratio.

(14) Frenz, B. *Enraf-Nonius Structure Determination Package*; Delft University Press: Delft, The Netherlands, 1982.
(15) Kutoglu, A.; Allmann, R. *Neues Jahr. Mineral., Monatsh.* **1972**, *8*, 339.
(16) Brec, R.; Ouvrard, G.; Evain, M.; Grenouilleau, P.; Rouxel, J. *J. Solid State Chem.* **1983**, *47*, 174.
(17) Evain, M.; Brec, R.; Ouvrard, G.; Rouxel, J. *J. Solid State Chem.* **1985**, *56*, 12.

Table V. Main Interatomic Angles (deg) and Distances (pm) in $CuVP_2S_6$

P-S1	202.7 (4)		
P-S2	202.8 (4)		
P-S3	203.0 (2)		
$P-S_{av}$	202.8		
P-P	216.8 (3)		
V-S1 (×2)	246.1 (3)	S1-V-S1	96.0 (2)
V-S2 (×2)	246.8 (1)	S1-V-S2 (×2)	82.43 (8)
V-S3 (×2)	247.3 (3)	S1-V-S2 (×2)	101.17 (8)
$V-S_{av}$	246.7	S1-V-S3 (×2)	82.56 (5)
		S2-V-S3 (×2)	94.26 (9)
		S2-V-S3 (×2)	82.28 (8)
		S3-V-S3	99.1 (2)
Cu1-S1	247 (2)		
Cu1-S2	257 (3)		
Cu1-S2	264 (3)		
Cu1-S3	267 (3)		
Cu1-S3	273 (3)		
Cu1-S1	288 (2)		
Cu2-S1	212.8 (4)	S1-Cu2-S2	119.1 (3)
Cu2-S2	212.7 (6)	S1-Cu2-S3	118.8 (3)
Cu2-S3	212.9 (7)	S2-Cu2-S3	118.6 (1)
Cu3-S1	227 (2)	S1-Cu3-S1	112.2 (7)
Cu3-S2	222 (2)	S1-Cu3-S2	109.7 (9)
Cu3-S3	226 (2)	S1-Cu3-S3	107.9 (8)
Cu3-S1	240 (2)	S1-Cu3-S2	108.5 (8)
		S1-Cu3-S3	109.0 (10)
		S2-Cu3-S3	109.6 (7)

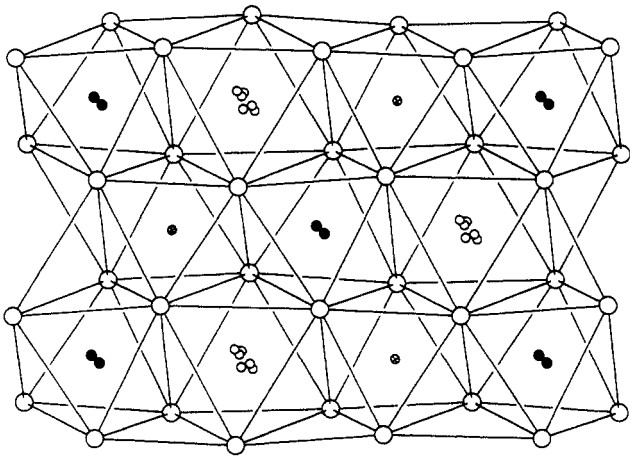

Figure 2. Triangular cationic arrangement in the two-dimensional sheet (*ab* plane) of the $CuVP_2S_6$ phase (black circle represents P, crossed circle represents V, small circle represents Cu, large circle represents S).

coordinates. Within errors the results were the same, which did not allow the establishment of the correct compound chirality.

Structure Description

The structure of $CuVP_2S_6$ (Figure 2) is to be compared to that of other $M^IM^{III}P_2S_6$ phases with a triangular cationic arrangement (i.e., $AgVP_2Se_6$, $AgScP_2S_6$, and $AgInP_2S_6$) and more closely to that of $CuCrP_2S_6$. If the various cationic arrangements (vide supra) are put aside, the $M^IM^{III}P_2S_6$ structure is based upon a close packing of layered arrays of sulfur atoms. In between every other layer, in octahedral sites, sit M^I and M^{III} cations and (P_2) pairs; in other words, the structure can be described as a succession of ($S_3M^IM^{III}P_2S_3$) slabs separated by van der Waals gaps. The sulfur stacking can be of the $(AB)_n$ or $(ABC)_n$ type; the cation stacking may also differ from one phase to another and introduce a doubling of the *c* periodicity (so far, no explanation was given for that). The systematically observed emptiness of the gaps, other than any afterward performed chemical intercalation, confers the material a truly two-dimensional (2D) character.

The $CuVP_2S_6$ structure follows the general pattern, and the stacking is of the $(ABC)_n$ type. The observed phosphorus to phosphorus and phosphorus to sulfur distances (d_{P-P} = 216.8 (3) pm and $d_{P-S(av)}$ = 202.8 pm) compare well with that of $V_{0.78}PS_3$

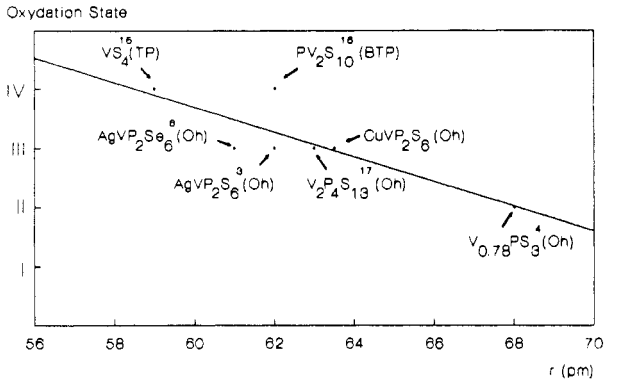

Figure 3. Vanadium ionic radius (pm) vs oxidation state in various thiophosphates and sulfides (TP = trigonal prismatic, BTP = bicapped trigonal prismatic, Oh = octahedral).

(d_{P-P} = 216.0 (3) pm and $d_{P-S(av)}$ = 202.8 pm.[4] Furthermore, the average vanadium to sulfur distance (246.7 pm) of the former phase is in good agreement with that obtained in the latter (250.4 pm). The slight difference between those two last average values accounts for the presence of vanadium(III) in one case and of a mixed-valence vanadium(III)/vanadium(II) in the other one, V^{II} ions being larger than V^{III} ions. It can also be noted the rather small dispersion of the vanadium to sulfur distances (246.1 (3), 246.8 (1), and 247.3 (3) pm); one might probably rule out any Jahn-Teller distortion as that supposed in $AgVP_2S_6$.[5] In that last compound, the strong distortion of the octahedra could have been attributed to the large cationic size difference as well. Considering $r(S^{2-})$ = 184 pm, a value of r = 63 pm is calculated for the ionic radius of vanadium(III). That value fits perfectly in the vanadium ionic radius versus oxidation-state curve deduced from all known thiophosphates and sulfides (Figure 3).

The least-squares refinement, in a split model description of the structure, led to the introduction of three kinds of copper sites in, or close to, each octahedron that normally corresponds to an M^I location: Cu1 near the center of the octahedron, Cu2 close to two of its triangular faces, and Cu3 on the outside toward the center of the adjacent tetrahedron in the van der Waals gap (Figure 4). The distribution is quite different from that reported for $CuCrP_2S_6$, for which only two split positions have been noted, both inside the M^I octahedron.[2] In addition, the occupancy factors had to be fixed in the $CuCrP_2S_6$ structure refinement. They were freed in the present work and converged toward proper values, since the total amount of copper (0.94 (3)) equals, in a 3σ range, the value of 1 expected from the elemental analysis and from a charge equilibrium point of view. In opposition, a common feature of both structures is the high values of the mean-square amplitudes of vibration (U_{ij}). In $CuVP_2S_6$, as in $CuCrP_2S_6$, all copper atoms present large U_{33} values, which implies either a static distribution of copper atoms along the octahedron 3-fold axis perpendicular to the slabs (e.g., parallel to the c^* parameter), a dynamic disorder, or a mixture of both.

Cu1 is near a 2-fold axis (on the axis, it would be at the very center of the sulfur octahedron). It follows a distribution of copper to sulfur distances (247, 257, 264, 267, 273, and 288 pm). This is slightly different from the situation in $CuCrP_2S_6$ where one can distinguish two groups of distances: three short ones (247.4, 253.2, and 253.7 pm) and three long ones (272.7, 272.9, and 287.3 pm). The occupation ratio and the U_{ij} thermal parameters of $CuVP_2S_6$'s Cu1 match those of $CuCrP_2S_6$'s CuB (the $CuCrP_2S_6$'s CuB occupation ratio was estimated and not refined).

Thrown off center, Cu2 atom sits near the octahedral triangular face, as the sulfur-copper-sulfur angles (118.6°, 118.8°, and 119.1°) indicate. Nevertheless, it remains inside the M^I octahedron, 23 pm off the face, with copper to sulfur distance values of 212.7, 212.8, and 212.9 pm. Once again, these values correspond to what was found in $CuCrP_2S_6$. However, its U_{33} parameter is a bit smaller than the corresponding $CuCrP_2S_6$'s CuA U_{33} (0.148×10^4 versus 0.171×10^4 pm^2); this suggests an undetected copper position (corresponding to Cu3, vide infra) in the

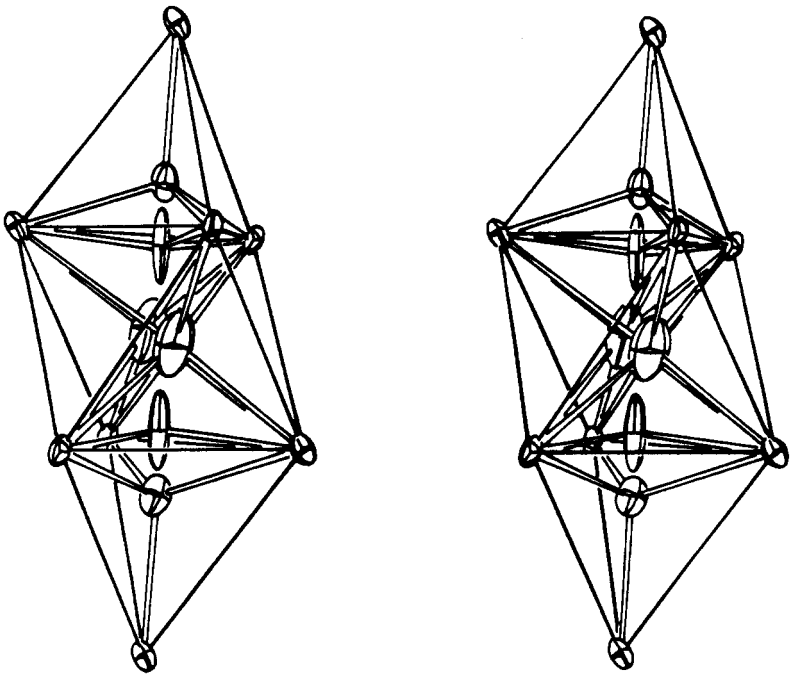

Figure 4. Stereographic view of the M^{I} octahedral site in $CuVP_2S_6$.

$CuCrP_2S_6$ structure refinement (that missing site being then presumably taken care of by a larger thermal vibration of CuA atoms). With 56.4% of the total amount, Cu2 is the major copper position.

The last copper position, Cu3, is located outside the M^{I} octahedra, in the van der Waals gap, and approximately on the Cu1–Cu2 axis. It stands in a tetrahedron site that shares a triangular face with the M^{I} octahedron. Two sets of distances (three short, 222, 226, and 227 pm, and one long, 240 pm) are calculated; nevertheless, Cu3 is positioned on the tetrahedron center, as confirmed by the S–Cu3–S angles (≈109.5°). The observed tetrahedral elongation is a common trend of all $M_2P_2S_6$ phases.[18] For instance, in $Fe_2P_2S_6$ one calculates two center-to-sulfur distance classes (3 × 211.4 and 1 × 251.5 pm) for each empty interslab tetrahedral site. This is to be related to the widening, in the $M_2P_2S_6$ phases, of the usual MX_2 van der Waals gap. Cu3 is the smallest contribution (e.g., 14.0%) to the total copper sum; nevertheless, it is a well-defined position with the smallest equivalent thermal factor among the copper atoms (B_{eq} = 2.3 × 10^4 pm^2) and with well-matched U_{ii} parameters.

The progression 213 pm → 229 pm → 266 pm of the average copper(I) to sulfur distances in triangular, tetrahedral, and octahedral sites, respectively, relates quite well with the progression 247 pm → 262 pm → 281 pm[19,20,4] of the observed average silver(I) to sulfur distances in similar environments.

Discussion

Octahedral environments are quite unusual for copper(I). Indeed, with a $3d^{10}4s^0$ configuration, copper atoms prefer either a linear or a tetrahedral surrounding. In chalcogenides, the latter one is largely preponderant. This is the case in spinel frameworks and in blende- or wurtzite-derived structures.[21] It is the same situation when copper(I) species occupy MX_2 van der Waals gaps in ternary Cu–MX_2 phases.[22] In the $M^{I}M^{III}P_2S_6$ phases, such an environment is a priori possible within and in between the $(S_3M^{I}M^{III}P_2S_3)$ slabs. The first case would imply by far too short copper to vanadium and copper to phosphorus distances; it thus must be discarded. The second would require vacancies on one-third of the intraslab octahedral sites; this does not seem in favor of the overall Coulombic stability of the phase (a confirmation, by network energy calculation of simulated possibilities, is in progress).

A simultaneous presence in some M^{I} octahedra of two copper atoms, as (Cu_2S_6) entities, can also be considered: this was the conclusion of a study on a partially substituted $M^{I}M^{III}P_2S_6$ phase, $Cu_{0.26}Mn_{0.87}P_2S_6$, for which the observed stoichiometry suggested such bimetallic groups.[22] Unfortunately, in that study, because of the disordered nature of the substitution and due to some inconsistencies between X-ray diffraction and EXAFS data, the real location of copper intraslab atoms remains uncertain. In addition, the suggested copper to copper distance (321 pm) does not match any of our calculated distances (d_{Cu-Cu} = 274 pm).

To elucidate the complex site distribution of copper atoms in $CuCrP_2S_6$, an EXAFS study was carried out on that phase.[23] The conclusions are not clear-cut. The authors calculated a Cu–S distance dispersion (σ = 4 pm) smaller than that of the Cr–S distance (σ = 6 pm) although the chromium positions are well defined (full local site occupancy and U_{ij}(max) = 0.0108 × 10^4 pm^2) and located in almost undistorted octahedra (Cr–S distance ranges from 243.2 to 245.6 pm) when compared to the copper position (statistical distribution and U_{ij}(max) = 0.1709 × 10^4 pm^2). In addition, they calculated 4.1 sulfur neighbors for each chromium found in an octahedral surrounding in the X-ray determination.

The copper to sulfur distances (222 pm) calculated from EXAFS data from both the $CuCrP_2S_6$ and $Cu_{0.26}Mn_{0.87}P_2S_6$ phases correspond to the tetrahedral copper to sulfur Cu3–S short distances (225 pm in average) rather than to the triangular Cu2–S shorter distances (212.8 pm in average). This result strengthens the above hypothesis of a possible tetrahedral Cu3 site in $CuCrP_2S_6$. High CuA and CuB σ values, in relation to high U_{33} values (0.171 × 10^4 and 0.089 × 10^4 pm^2, respectively), can explain the absence of corresponding signals in EXAFS data.

It is worth noticing that the copper ions largely perturb the sulfur triangular arrangement. This is particularly obvious when one considers the S–S distances of the two facing triangles that constitute the Cu, P_2, and V octahedra. In $Fe_2P_2S_6$, the average S–S distance (341.5 pm) in the triangles that sandwich a P_2 pair

(18) Brec, R. *Solid State Ionics* **1986**, *22*, 3.
(19) Evain, M.; Boucher, F.; Brec, R.; Mathey, Y. *J. Solid State Chem.*, to be published.
(20) Shannon, R. D. *Structure and Bonding in Crystals*; O'Keeffe, M., Navrotsky, A., Eds.; Academic Press: New York, 1981; Vol. 2, p 61.
(21) Subba Rao, G. V.; Shafer, M. W. *Physics and Chemistry of Materials with Layered Structures*; Levy, F. A., Ed.; R. Reidel Publishing Co.: Dordrecht, The Netherlands, 1979; Vol. 6, p 182.
(22) Mathey, Y.; Michalowicz, A.; Toffoli, P.; Vlaic, G. *Inorg. Chem.* **1984**, *23*, 897.
(23) Mathey, Y.; Mercier, H.; Michalowicz, A.; Leblanc, A. *J. Phys. Chem. Solids* **1985**, *46*, 1025.

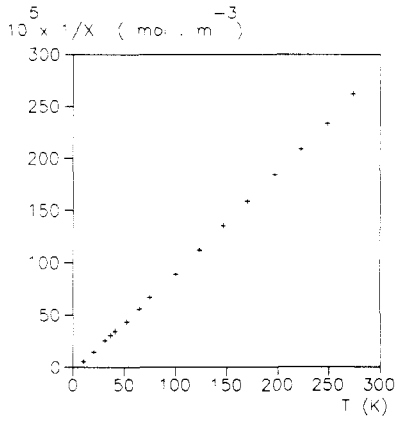

Figure 5. Reciprocal molar magnetic susceptibility (corrected for core magnetism) vs temperature of $CuVP_2S_6$ in the range 5–298 K.

is comparable to that (344.3 pm) found in the two three-cornered units surrounding Fe cations. In $V_{0.78}PS_3$, the former distance is conserved (341.5 pm) and the latter slightly reduced (337.3 pm) in relation with the smaller size of V^{II} and the presence of V^{III}. In the title compound, if the triangular, average S–S distance remains, once again, the same in P_2 octahedra (340 pm), it shrinks to 326 pm on the V^{III} site and expands to 375 pm around the Cu^{I} position (see Figure 2). The sulfur framework is flexible enough to accommodate various atomic localizations and sizes. The rearrangement can occur in the triangular faces shared by neighboring octahedra (situation in $AgCrP_2S_6$[4] and in $AgVP_2S_6$,[3] where the large Ag^{I} ions occupy the center of the octahedra and constitute infinite zigzag chains) or in the gap-bordering triangles (situation in the present study and in $Ag_2MnP_2S_6$[19]).

Magnetic Properties

Susceptibility measurements were carried out on a Faraday balance apparatus in the 5–298 K temperature range; only powder samples, obtained from bulk material after removal of Cu_3PS_4 surface impurities, were studied. In Figure 5 is reported the temperature dependence of the reciprocal molar magnetic susceptibility ($1/\chi_{mol}$) corrected for diamagnetic contribution. In the whole temperature range, $1/\chi_{mol}$ obeys the Curie–Weiss law, $1/\chi_{mol} = (T - \theta_p)/C_{mol}$, where C_{mol} and θ_p are the molar Curie constant and the Weiss constant, respectively. The molar Curie constant ($C_{mol} = 10.4 \times 10^{-6}$ $m^3 \cdot K \cdot mol^{-1}$) almost match the calculated spin-only value of V^{III} ions (12.5×10^{-6} $m^3 \cdot K \cdot mol^{-1}$). The Weiss constant ($\theta_p \approx 6$ K) is positive (i.e., the predominant magnetic interactions are of the ferromagnetic type and very weak). Of the eight V^{III} neighbors each vanadium ion sees, the closest six in its own layer ($d_{V-V} = 595$ pm) generate positive interactions ($J_{intra} > 0$) and thus govern the Weiss constant sign whereas the two remaining ones, in different slabs (above and below, respectively) and at longer distances ($d_{V-V} = 669$ pm), are too far to be able to induce magnetic interslab coupling at low temperature.

Conclusion

The quest for novel $M^{I}M^{III}P_2S_6$ phases with promising physical properties led to the preparation of a new material: $CuVP_2S_6$. If a straightforward synthesis of the pure bulk is not achieved yet, the atomic structure could be solved and investigated on the basis of a split atom model description. The distribution of copper(I) cations on various sites (e.g., octahedra, triangles, and tetrahedra) and the large calculated thermal parameters suggest several possibilities. One of them is the occurrence of several microdomains, each containing one type of coordination, as already suggested for $CuCrP_2S_6$.[9] Another could be related to copper diffusion from one site to another, with a time of location in some of the crystal sites long enough to be considered as specific atomic positions by the X-ray technique. This suggests that different copper distributions with respect to temperature may take place and possibly give rise to various $CuVP_2S_6$ polymorphs. For instance, a Raman study revealed a shift of copper from one tetrahedral site to another in $Cu_{0.26}Mn_{0.87}PS_3$.[24] A single crystal structure study on $AgCrSe_2$ versus temperature[25] also showed a second-order transition, investigated through anharmonic thermal vibrations. Such experiments, along with site potential calculations, are presently carried out to better understand the structure of $CuVP_2S_6$.

A comparison of $CuVP_2S_6$ (and also $CuCrP_2S_6$) with the parent silver phases shows that copper(I) is much less stable in an octahedral sulfur site than silver(I) is. Both cations, however, present very high thermal factors, evidencing a problem of stability in their sites. This may be related to the following hypothesis: If one considers a layer $M_2P_2S_6$ compound, the substitution of M^{II} by M^{I} and M^{III} cations implies the filling of the octahedral sites of the close packing. Although Cu(I) and Ag(I) would probably prefer a tetrahedral environment, the site potential seems strong enough to attract all or part of the monovalent cations in the intraoctahedral voids. However, there seems to be a competition between this Coulombic attraction and the specific coordination cation stability. The observed site distribution may be related to these factors, to which one may add the possible occurrence of a Jahn–Teller effect[7] explaining the off-center positions of Cu(I) and Ag(I). The possibility of shifting from one position to another is also to be related to the polarizability of the moving M^{I} cation.

Temperature and bond ionicity changes should allow to modulate the occupancy ratio of the copper (silver) sites. In particular, less ionic phases (selenides) should favor triangular and tetrahedral positions.

Supplementary Material Available: Tables of complete crystallographic data, bond distances and bond angles, anisotropic thermal parameters, and root-mean-square amplitudes of anisotropic displacements (7 pages); a table of observed and calculated structure factors (7 pages). Ordering information is given on any current masthead page.

(24) Mathey, Y.; Clément, R.; Audiere, J. P.; Poizat, O.; Sourisseau, C. *Solid State Ionics* **1983**, *9–10*, 459.
(25) Van der Lee, A.; Wiegers, G. A. *J. Solid State Chem.* **1989**, *82*, 216.